Silent phase qubit based on *d*-wave Josephson junctions

M. H. S. Amin,[1] A. Yu. Smirnov,[1] A. M. Zagoskin,[1,2] T. Lindström,[3] S. A. Charlebois,[4] T. Claeson,[3] and A. Ya. Tzalenchuk[5]
[1]*D-Wave Systems Inc., 320-1985 Broadway, Vancouver, British Columbia, V6J 4Y3, Canada*
[2]*Physics and Astronomy Department, The University of British Columbia, 6224 Agricultural Road, Vancouver, British Columbia, V6T 1Z1, Canada*
[3]*Microtechnology and Nanoscience, Quantum Device Physics Laboratory, Chalmers University of Technology and Göteborg University, SE-412 96 Göteborg, Sweden*
[4]*Département de génie électrique et de génie informatique, Université de Sherbrooke, 2500, boulevard Université, Sherbrooke, Québec, J1K 2R1, Canada*
[5]*National Physical Laboratory, Queens Road, Teddington, Middlesex TW11 0LW, United Kingdom*
(Received 7 July 2004; published 24 February 2005)

A flux qubit is designed and fabricated that capitalizes on intrinsic properties of submicron YBCO (yttrium-barium-copper oxide high-T_c superconductor) grain boundary junctions. The operating point is protected from the fluctuations of the external fields, already on the classical level. The effects of external perturbations only appear in the third or fourth order, depending on the character of the coupling. The estimates of the decoherence due to fluctuations of the external flux show that an experimental observation of coherent quantum tunneling and Rabi oscillations in the system is feasible.

DOI: 10.1103/PhysRevB.71.064516 PACS number(s): 74.50.+r, 85.25.−j, 74.72.−h, 74.78.Na

I. INTRODUCTION

Over the last few years a series of experiments[1–3] provided conclusive evidence of quantum superposition in mesoscopic and macroscopic superconductors. The task at hand is scaling up of the system, with two goals in mind: to probe how far quantum superposition can be pushed into the macroscopic world and to develop an element base for quantum computing, which only becomes viable on the scale 10–100 qubits.

It was suggested that use of high-T_c cuprates in qubits would dispose of the need to apply fine-tuned external fields to keep it in the operating point, due to the time-reversal symmetry breaking in systems with DD junctions.[4,5] On the level of a few qubits this is not a major advantage, compared to the relative difficulty of fabrication and threat of extra decoherence from nodal quasiparticles and zero-energy states (ZESs) in cuprates. Therefore the research was concentrated on conventional superconductors, where all of the aforementioned successes were achieved.

Nevertheless, the logical progression of research from single qubit to qubit-qubit coupling and further to qubit registers is bringing us to the point where intrinsic bistability of high-T_c qubits will become a major advantage. In the last few years, we saw the development of reliable fabrication of bistable submicron high-T_c structures.[6–8] Theoretical estimates[9,10] showing that the decoherence from ZES and nodal quasiparticles may be significantly overestimated, and recent experimental demonstration of macroscopic quantum tunneling in biepitaxial YBCO (yttrium-barium-copper oxide high-T_c superconductor) junctions[11] make further effort in this direction relevant.

In this paper we report on the design and fabrication of a type of flux qubit that capitalizes on intrinsic properties of submicron YBCO grain boundary junctions. The advantage of the design is that the operating point is protected from the fluctuations of the external fields, already on the classical level. Our estimates of the decoherence due to fluctuations of the external flux show the feasibility of an experimental observation of coherent quantum tunneling and Rabi oscillations in the system.

II. QUBIT DESIGN

The "silent qubit" (for the etimology, see below) can be viewed as a dc superconducting quantum interference device (SQUID) formed out of high-T_c film, with two DD-grain boundary junctions defining a mesoscopic island [Figs. 1(a) and 1(c)]. The crystal lattice and *d*-wave order parameter orientations on the two sides of the grain boundary are chosen in such a way that each junction has a doubly degenerate ground state.[6,12]

To simplify the analysis, we keep only two harmonics in the current-phase relations of the DD junctions

$$I_i = I_{ci} \sin \phi_i - I'_{ci} \sin 2\phi_i, \tag{1}$$

where I_{ci} is the critical current and ϕ_i is the phase difference across the ith junction ($i=1,2$). This approximation successfully reproduces the observed behavior of similar devices in the classical regime.[6,8] The flux quantization condition relates the phases ϕ_1 and ϕ_2 to the total flux through the loop Φ via

$$\phi \equiv \phi_1 + \phi_2 = 2\pi \frac{\Phi}{\Phi_0},$$

where $\Phi_0 = h/2e$ is the flux quantum. Introducing the superconducting phase of the island

$$\theta \equiv \frac{\phi_1 - \phi_2}{2},$$

the free energy of the qubit, threaded by an external magnetic flux Φ_x, in units of the Josephson energy E_J ($\equiv E_1$, where $E_i = I_{ci}\Phi_0/2\pi$), is given by

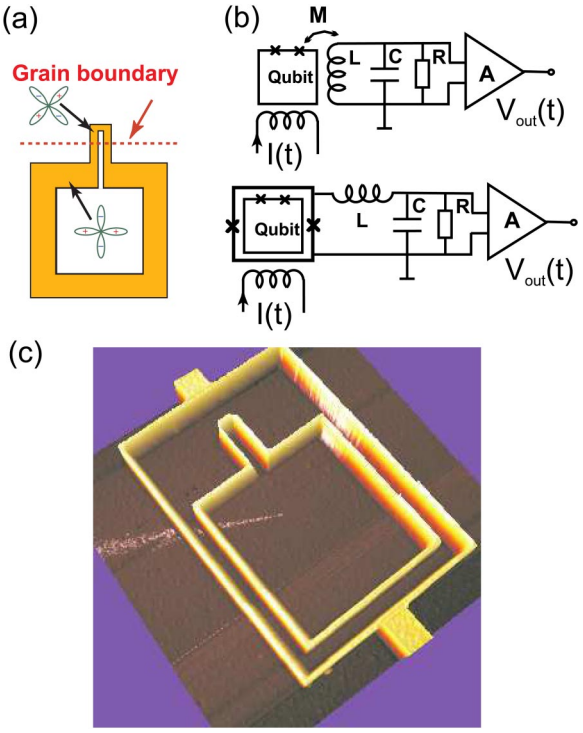

FIG. 1. (a) (Color online) "Silent" qubit. The dashed line shows the location of the grain boundary junction. (b) For the decoherence measurements and readout the qubit can be coupled to the tank inductively through a pickup coil (Ref. 17) or a dc SQUID (Ref. 19). Using the approach of (Ref. 17), the Rabi decay time can be determined from the spectral density of voltage fluctuations in the low-frequency resonant tank in the presence of weak driving rf signal applied to the qubit. (c) AFM picture demonstrating the possibility of fabrication of the proposed qubit and readout dc-SQUID out of YBCO on an $SrTiO_3$ bicrystal substrate.

$$\mathcal{U}(\theta,\phi)=\frac{(\phi-\phi_x)^2}{2\beta_L}-\mathcal{E}_\phi\left[\cos\theta-\frac{\tilde{\alpha}_\phi}{4}\cos(2\theta)\right]+\tilde{\mathcal{U}}(\theta,\phi). \tag{2}$$

Here

$$\alpha_i=2I'_{ci}/I_{ci},\quad \mathcal{E}_\phi=(1+\eta)\cos(\phi/2),$$

$$\tilde{\alpha}_\phi=\frac{(\alpha_1+\eta\alpha_2)\cos\phi}{(1+\eta)\cos(\phi/2)},\quad \eta=E_2/E_1,$$

and $\phi_x=2\pi\Phi_x/\Phi_0$. The dimensionless self-inductance of the loop

$$\beta_L\equiv 2\pi\frac{LI_{c1}}{\Phi_0}$$

is considered negligible ($\beta_L\to 0$); then $\phi\to\phi_x$ and the first term in Eq. (2) can be dropped.

The last term in Eq. (2)

$$\tilde{\mathcal{U}}(\theta,\phi)=-\left[\eta-1+(\alpha_1-\eta\alpha_2)\cos\frac{\phi}{2}\cos\theta\right]\times\sin\frac{\phi}{2}\sin\theta \tag{3}$$

is zero when the two junctions are identical (i.e., $\eta=1$ and $\alpha_1=\alpha_2$). In this case the potential energy minima are at

$$\theta=\pm\arccos\left(\frac{1}{\tilde{\alpha}_\phi}\right).$$

when $\tilde{\alpha}_\phi>1$ and zero otherwise. The $\pm$ signs correspond to the states on the right and left sides of the potential well (i.e., $|\pm\rangle$), respectively. For $\tilde{\alpha}_\phi>1$ the potential has two minima, which are degenerate at *any* external flux ϕ_x. The current induced in the loop by the external flux does *not* depend on the state of the qubit, which justifies the moniker "silent." The potential profile (2) is similar to the one of a persistent current qubit,[2] but here we have only one independent phase (as $\beta_L\to 0$), and the problem becomes one-dimensional. The barrier between the potential minima is flux dependent:

$$W=\cos(\phi_x/2)(\tilde{\alpha}_\phi+\tilde{\alpha}_\phi^{-1}-2).$$

In the general case ($\alpha_1\neq\alpha_2,\eta\neq 1$) the two minima are only degenerate when $\phi_x=0$. Now a *state-dependent* persistent current flows in the loop even in zero external field; in units of I_{c1},

$$\mathcal{I}_0^\pm=\pm[\eta\sqrt{\tilde{\alpha}_0^2-1}/(1+\eta)\tilde{\alpha}_0^2](\alpha_2-\alpha_1),$$

where $\tilde{\alpha}_0\equiv\tilde{\alpha}_{\phi=0}$.

The intermediate regime ($\alpha_1=\alpha_2,\eta\neq 1$) is most interesting. It takes place when junctions have similar current-phase dependencies, but different critical currents (i.e., widths), and should be expected if the junctions are close enough to each other (Fig. 1). At $\phi_x=0$, the equilibrium value of θ is the same for both junctions, and there is no spontaneous current $\mathcal{I}_0^\pm=0$. At finite ϕ_x, the induced currents differ for the two states of the qubit, but the difference is of higher order in ϕ_x, keeping the qubit silent.

Expanding the free energy to the third order in ϕ_x, we find for the minima

$$\mathcal{U}_{\min}^\pm=A_0+A_2\phi_x^2\pm A_3\phi_x^3, \tag{4}$$

where A_i are explicit functions of $\tilde{\alpha}_0$ and η (see the Appendix). As expected, there is no first order dependence on ϕ_x ($A_1=0$). The second order term in Eq. (4) does not depend on the state of the qubit. The first state-dependent term in the minimum energy of the system is $O(\phi_x^3)$ (Fig. 2). Therefore small fluctuations of ϕ_x do not affect the degeneracy of the states. The difference between the energy minima grows as the external flux is increased until the point at which the potential barrier vanishes altogether and the minimum with higher energy disappears (the jumps in Fig. 2).

The current in the loop is found from

$$\mathcal{I}_\phi^\pm=\partial_{\phi_x}\mathcal{U}_{\min}^\pm=2A_2\phi_x\pm 3A_3\phi_x^2.$$

This current generates a state-dependent magnetic flux

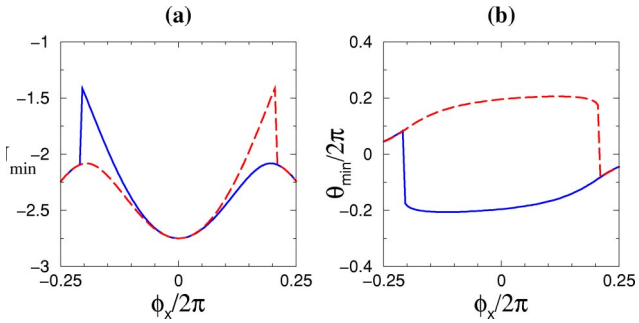

FIG. 2. (Color online) The minimum of the free energy (a) and the corresponding values of θ at the minimum points (b) as a function of ϕ_x, for $\eta=2$ and $\alpha_1=\alpha_2=3$. The solid (blue) and dashed (red) lines correspond to the $|-\rangle$ and $|+\rangle$ states, respectively.

$$\delta\phi \equiv \phi - \phi_x = \beta_L \mathcal{I}_\phi^\pm.$$

Note, that the state-dependent contribution to the induced flux is $O(\phi_x^2)$. For a finite self-inductance β_L, $\delta\phi$ has to be calculated self-consistently. Figure 3 shows the result of such a calculation. With the parameters chosen, an external flux close to $0.2\ \Phi_0$ generates an additional flux ($\sim 0.005\ \Phi_0$) through the loop, which is of the same order as the estimate based on the above expansion.

Tunneling between the potential minima occurs due to the uncertainty relation between the charge Q of the island and its superconducting phase θ. The tunneling matrix element is approximately given by ($\hbar=k_B=1$)

$$\Delta \approx \omega_p(\phi_x) e^{-\sqrt{\zeta W(\phi_x) E_J/E_C}}, \tag{5}$$

where ζ is a constant of the order of 1, $E_C=e^2/2C$ is the charging energy, and C is the effective capacitance of the junctions. The coefficient $\omega_p(\phi_x) \equiv \sqrt{\omega_p^+ \omega_p^-}$ is determined by the frequencies $\omega_p^\pm$ of small oscillations in the right and left potential minima, respectively. This dependence follows from the expression of Δ as the matrix element between the lowest energy states in the two wells. It is only valid qualitatively in the case of $\tilde{\alpha}_0 \sim 1$ (see Ref. 13). Due to the symmetry of the potential profile when $\alpha_1=\alpha_2$, the terms of the first order in ϕ_x cancel, and we are left with

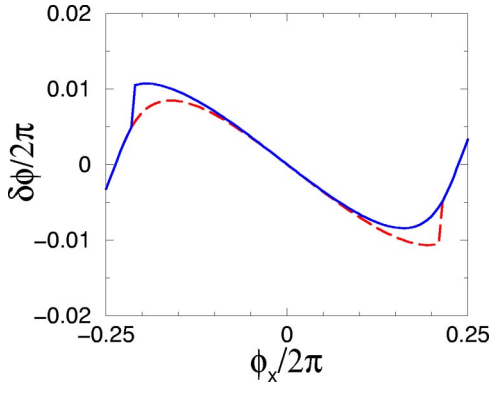

FIG. 3. (Color online) Self-consistent calculation of the self-generated flux for the system of Fig. 2, with $\beta_L=0.01$. The solid (blue) and dashed (red) lines correspond to the $|-\rangle$ and $|+\rangle$ states, respectively.

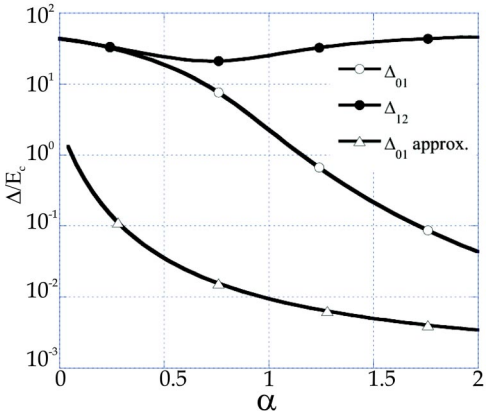

FIG. 4. Evolution of Δ_{01} and Δ_{12} (the gap between the two lowest excited levels) with respect to the parameter $\alpha=\alpha_1=\alpha_2$ (numerical results). Numerical results are compared with the approximation (5).

$$\omega_p(\phi_x) = \sqrt{E_J E_C(\alpha_0 - \alpha_0^{-1})}(1 - \kappa\phi_x^2),$$

where κ is a dimensionless coefficient of $O(1)$. Fluctuations of ϕ_x influence W and therefore Δ. Expanding the Josephson potential near the origin, we obtain the tunneling barrier

$$W = \mathcal{U}_{\max} - \mathcal{U}_{\min}^\pm = (B_0 - A_0) + (B_2 - A_2)\phi_x^2 + O(\phi_x^3) \tag{6}$$

(see the Appendix). Again there is no dependence on ϕ_x in the first order.

The numerical diagonalisation of the Hamiltonian, for $\phi_x=0$ and for arbitrary $\tilde{\alpha}_0$ using Eq. (2), demonstrates the increased anharmonicity of the system[13] (Fig. 4). As $\tilde{\alpha}_0$ approaches 1, the two lowest (working) levels in the double well converge almost exponentially, while the energy gap separating them from the next excited level remains nearly constant. The spacing Δ between the working levels can therefore be tuned using $\tilde{\alpha}_0$ while keeping them effectively decoupled from the other levels of the well.

This justifies truncating the Hilbert space of the qubit to the two lowest energy states, which yields the effective Hamiltonian

$$H = \tfrac{1}{2}\Delta(\phi_x)\sigma_x + \tfrac{1}{2}\epsilon(\phi_x)\sigma_z, \tag{7}$$

where $\epsilon(\phi_x) \approx E_J A_3 \phi_x^3$. All single qubit operations can be realized by applying controlled flux ϕ_x. Note that the qubit only leaves the operating point when a finite external flux is applied. Unlike the earlier qubit designs[2,3] this point is protected from external flux fluctuations already on the classical level, due to the qubic $\epsilon(\phi_x)$ [see Eq. (4)].

III. IMPLEMENTATION

The implementation of the novel qubit design requires the second harmonic of the critical current [Eq. (1)] to be comparable to the first. Such a situation is expected in 0/45° tilt grain boundary junctions between *d*-wave superconductors,

where the first harmonic is suppressed by symmetry.[14] Recent work on 0/45° grain boundary YBCO junctions reported current-phase relations with second harmonic components.[6,13] The techniques used in Refs. 8 and 15 allow a measurement of $\tilde{\alpha}_0$ above 0.1. The experiments have revealed values of $\tilde{\alpha}_0$ of the order 1 consistent with the requirements of the current design.

Other parameters such as the critical current magnitude, the junction capacitance and, the SQUID loop inductance are also relevant for the qubit operation. We have shown in Ref. 13 that it is possible to fabricate 300-nm-wide grain boundary junctions with critical currents ~ 0.5 μA and capacitance of 10 fF. SQUID loops with inductance of order 10 pH (10×10 μm^2) were fabricated of YBCO on $SrTiO_3$. To achieve such results, the thin YBCO film grown by pulsed laser deposition is patterned by ion milling through an amorphous carbon mask. The etching mask with submicron structures is obtained by a standard electron beam lithography technique.

The readout of a flux qubit is based on detection of the magnetic flux produced by a quantum state-dependent persistent current flowing in the loop. One way to do it is to couple the qubit to a current-biased dc SQUID and use the switching of the latter to the resistive regime to distinguish between the states of the qubit. Recently, such an approach was employed to observe coherent oscillations in an aluminum persistent-current qubit.[2] Its drawback is the extension of its advantages, a rather strong coupling of the qubit to the readout circuit, which may be responsible for comparatively short decoherence time in Ref. 2. Our design seems well suited for this technique, due to a better intrinsic protection from the external noise sources.

Another way of observing the quantum dynamics of a flux qubit is to couple it to a high-quality *LC* circuit and monitor the magnetic susceptibility of the latter, which depends on the state of the qubit.[16] This method was used to demonstrate Rabi oscillations[17] and two-qubit entanglement.[18] It allows long decoherence times, but time-domain operations on a qubit are impeded. Recently, a hybrid approach was realized,[19,20] where the pickup coil of the *LC* circuit was replaced with a dc SQUID.

For the sample of Fig. 1(c) we fabricated the readout SQUID in the same high-T_c film as the qubit itself; alternatively it could be made of a low-T_c superconductor. If implemented with on-chip grain boundary junctions, one must take into account the presence of a second harmonic in the current-phase relation of the readout SQUID.[8]

IV. DISCUSSION

In order to show the feasibility of observation of coherent quantum tunneling and Rabi oscillations in our silent qubit, we will consider the best-case scenario, that is, assume the setup[16,17,21] [see Fig. 1(b)], where the qubit is coupled to a high-quality *LC* circuit.

The tank circuit has a resonance frequency ω_T and a damping rate γ_T. The mutual inductance is $M = k\sqrt{L_T L}$, $k \leqslant 1$ being the coupling coefficient, and L and L_T are the inductance of the qubit and tank, respectively.

Without limiting the generality of our approach, we can ascribe all the dephasing and dissipation in the qubit to its interaction with the fluctuating flux $\phi_x(t)$, created by the tank current $I_T(t)$. These fluctuations are characterized by the correlator

$$K(t,t') = \langle I_T(t), I_T(t') \rangle,$$

the spectral density

$$K(\omega) = \omega(\gamma_T \omega_T^2 / L_T) \frac{\coth(\omega/2T) + 1}{(\omega^2 - \omega_T^2)^2 + \gamma_T^2 \omega^2}$$

and the dispersion

$$\langle I_T^2 \rangle = K(t,t) = \frac{\omega_T}{2L_T} \coth \frac{\omega_T}{2T}.$$

At $\phi_x = 0$, the qubit Hamiltonian becomes

$$H = (\Delta/2)\sigma_x - \lambda_2 I_T^2 \sigma_x - \lambda_3 I_T^3 \sigma_z, \tag{8}$$

where $\lambda_{2,3}$ are coupling coefficients depending on the qubit parameters. In the Bloch-Redfield approximation,[22,23] we calculate the energy relaxation rate

$$\Gamma = 30 \lambda_3^2 \langle I_T^2 \rangle^2 \frac{\gamma_T}{\Delta^3} \frac{\omega_T^2}{L_T} \coth \frac{\Delta}{2T} \tag{9}$$

together with the dephasing time of the qubit γ^{-1}, where $\gamma = \Gamma/2 + \gamma_0$,

$$\gamma_0 = \frac{16\pi}{3} \lambda_2^2 \frac{\gamma_T^2 T^3}{L_T^2 \omega_T^4}$$

if $T \ll \omega_T$, and

$$\gamma_0 = \lambda_2^2 Q_T \frac{\omega_T}{L_T^2} \left[\coth^2 \frac{\omega_T}{2T} - 1 \right]$$

if $T \geqslant \omega_T$.

Using the experimental data of Ref. 13 ($I_c = 0.5$ μA, $I_c' = 0.6$ μA, $C \approx 10$ fF), we find $E_C \approx 2$ GHz, $\omega_p/2\pi \approx 40$ GHz, and $\Delta/2\pi \approx 1.6$ GHz. For $\beta_L \sim 0.01$, which is the value used in Fig. 3, the inductance of the loop is of the order of 10 pH. To estimate the contributions of the cubic and quadratic terms to qubit dephasing and dissipation, we chose the following parameters: $\eta = 2$, $\alpha_1 = \alpha_2 = 2.4$, and $E_J = 1.66 \times 10^{-22} J$. If the tank frequency is $\omega_T/2\pi = 10$ MHz, its quality factor $Q_T = 2000$, and the coupling coefficient $k \sim 1/33$, then contribution of *quadratic* flux fluctuations to dephasing rate is small, so that the dephasing time due to qubit coupling to the tank is $\gamma_0^{-1} \simeq 20$ ms at temperatures of order 10 mK, while the contribution of the *cubic* fluctuations to the dephasing and relaxation rates is totally negligible. It means that at the operating point the silent qubit is practically decoupled from the fluctuations caused by the controlling circuits. The dominant source of decoherence is from the nodal quasiparticles at the junction, considered in Ref. 9, which may reduce the decoherence time to about 1–100 ns. This is not in itself an unsurmountable obstacle, since very fast (2–5 ns) measurements of flux qubits were achieved.[20,24]

V. CONCLUSION

In conclusion, a flux qubit, using specific properties of submicron YBCO grain boundary junctions, was proposed

and fabricated. The symmetry of the device provides an operating point, which is intrinsically stable and protected against the external field fluctuations. Estimates show that observation of coherent quantum dynamics in the system is feasible using existing experimental techniques.

ACKNOWLEDGMENTS

We are grateful to A. Golubov, E. Il'ichev, F. Lombardi, A. Maassen van den Brink, Y. Nakamura, and A. Shnirman for stimulating discussions.

APPENDIX

The coefficients in Eqs. (4), (6), and (8) are as follows:

$$A_0 = -\frac{1}{4}(1+\eta)(\tilde{\alpha}_0 + 2\tilde{\alpha}_0^{-1}),$$

$$A_2 = \frac{\eta}{\eta+1}\frac{\tilde{\alpha}_0^2 - 1}{2\tilde{\alpha}_0},$$

$$A_3 = \frac{\eta(\eta-1)}{(\eta+1)^3}\frac{\sqrt{\tilde{\alpha}_0^2 - 1}}{2\tilde{\alpha}_0},$$

$$B_0 = -(\eta+1)(1-\tilde{\alpha}_0/4),$$

$$B_2 = -\frac{(\tilde{\alpha}_0 - 1)}{4}\frac{\eta}{(\eta+1)},$$

$$\lambda_2 = -\frac{\Delta}{4}\nu_0\left(\frac{2\pi M}{\Phi_0}\right)^2,$$

$$\lambda_3 = -E_J A_3\left(\frac{2\pi M}{\Phi_0}\right)^3,$$

$$\nu_0 = \frac{2\tilde{\alpha}_0 + \tilde{\alpha}_0^{-1}}{\tilde{\alpha}_0 - \tilde{\alpha}_0^{-1}} + \sqrt{\frac{\zeta W E_J}{E_C}}\frac{B_2 - A_2}{B_0 - A_0}.$$

[1] Y. Nakamura, Yu. A. Pashkin, and J. S. Tsai, Nature (London) **398**, 786 (1999); J. Friedman, V. Patel, W. Chen, S. K. Tolpygo, and J. E. Lukens, *ibid.* **406**, 43 (2000); J. M. Martinis, S. Nam, J. Aumentado, and C. Urbina, Phys. Rev. Lett. **89**, 117901 (2002); Y. Yu, S. Han, X. Chu, and Z. Wang, Science **296**, 889 (2002); A. J. Berkley, H. Xu, R. C. Ramos, M. A. Gubrud, F. W. Strauch, P. R. Johnson, J. R. Anderson, A. J. Dragt, C. J. Lobb, and F. C. Wellstood, *ibid.* **300**, 1548 (2003).

[2] I. Chiorescu, Y. Nakamura, C. J. P. M. Harmans, and J. E. Mooij, Science **299**, 1869 (2003).

[3] D. Vion, A. Aassime, A. Cottet, P. Joyez, H. Pothier, C. Urbina, D. Esteve, and M. H. Devoret, Science **296**, 889 (2002).

[4] L. B. Ioffe, V. B. Geshkenbein, M. V. Feigel'man, A. L. Fauchère, and G. Blatter, Nature (London) **398**, 679 (1999).

[5] A. Zagoskin, cond-mat/9903170 (unpublished); A. Blais and A. M. Zagoskin, Phys. Rev. A **61**, 042308 (2000).

[6] E. Il'ichev, M. Grajcar, R. Hlubina, R. P. J. IJsselsteijn, H. E. Hoenig, H.-G. Meyer, A. Golubov, M. H. S. Amin, A. M. Zagoskin, A. N. Omelyanchouk, and M. Yu. Kupriyanov, Phys. Rev. Lett. **86**, 5369 (2001).

[7] A. Ya. Tzalenchuk, T. Lindström, S. Charlebois, E. A. Stepantsov, and Z. Ivanov (unpublished).

[8] T. Lindström, S. A. Charlebois, A. Ya. Tzalenchuk, Z. Ivanov, M. H. S. Amin, and A. M. Zagoskin, Phys. Rev. Lett. **90**, 117002 (2003).

[9] M. H. S. Amin and A. Yu. Smirnov, Phys. Rev. Lett. **92**, 017001 (2004).

[10] Ya. V. Fominov, A. A. Golubov, and M. Yu. Kupriyanov, JETP Lett. **77**, 587 (2003).

[11] T. Bauch, F. Lombardi, F. Tafuri, A. Barone, G. Rotoli, P. Delsing, and T. Claeson (unpublished).

[12] M. H. S. Amin, A. N. Omelyanchouk, and A. M. Zagoskin, Phys. Rev. B **63**, 212502 (2001); M. H. S. Amin, A. N. Omelyanchouk, S. N. Rashkeev, M. Coury, and A. M. Zagoskin, Physica B **318**, 162 (2002).

[13] A. Ya. Tzalenchuk, T. Lindström, S. A. Charlebois, E. A. Stepantsov, Z. Ivanov, and A. M. Zagoskin, Phys. Rev. B **68**, 100501(R) (2003).

[14] A. A. Golubov, M. Yu. Kupriyanov, and E. Ilichev, Rev. Mod. Phys. **76**, 411 (2004).

[15] S. A. Charlebois, T. Lindström, A. Ya. Tzalenchuk, Z. Ivanov, and T. Claeson, Physica C **408–410**, 926 (2004).

[16] E. Il'ichev, A. Yu. Smirnov, M. Grajcar, A. Izmalkov, D. Born, N. Oukhanski, Th. Wagner, W. Krech, H.-G. Meyer, and A. M. Zagoskin, Fiz. Nizk. Temp. **30**, 823 (2004); cond-mat/0402559 (unpublished).

[17] E. Ilichev, N. Oukhanski, A. Izmalkov, Th. Wagner, M. Grajcar, H.-G. Meyer, A. Yu. Smirnov, A. Maassen van den Brink, M. H. S. Amin, and A. M. Zagoskin, Phys. Rev. Lett. **91**, 097906 (2003).

[18] A. Izmalkov, M. Grajcar, E. Ilichev, Th. Wagner, H.-G. Meyer, A. Yu. Smirnov, M. H. S. Amin, A. Maassen van den Brink, and A. M. Zagoskin, Phys. Rev. Lett. **93**, 037003 (2004).

[19] A. Lupascu, C. J. M. Verwijs, R. N. Schouten, C. J. P. M. Harmans, and J. E. Mooij, Phys. Rev. Lett. **93**, 177006 (2004).

[20] P. Bertet, I. Chiorescu, K. Semba, C. J. P. M. Harmans, and J. E. Mooij, cond-mat/0405024 (unpublished).

[21] M. Grajcar, A. Izmalkov, E. Il'ichev, Th. Wagner, N. Oukhanski, U. Huebner, T. May, I. Zhilyaev, H. E. Hoenig, Ya. S. Greenberg, V. I. Shnyrkov, D. Born, W. Krech, H.-G. Meyer, A. Maassen van den Brink, and M. H. S. Amin, Phys. Rev. B **69**, 060501(R) (2004).

[22] A. Yu. Smirnov, Phys. Rev. B **68**, 134514 (2003).

[23] Y. Makhlin and A. Shnirman, Phys. Rev. Lett. **92**, 178301 (2004).

[24] J. Claudon, F. Balestro, F. W. J. Hekking, and O. Buisson, Phys. Rev. Lett. **93**, 187003 (2004).